Research Article | Vol. 11, No. 7 / 1 July 2021 / Optical Materials Express 2326
Optical Materials EXPRESS

Non-Hermitian metasurfaces for the best of plasmonics and dielectrics

FRANK YANG, ALEXANDER HWANG, CHLOE DOIRON, AND GURURAJ V. NAIK*

Department of Electrical and Computer Engineering, Rice University, Houston, TX 77005, USA
**guru@rice.edu*

Abstract: Materials and their geometry make up the tools for designing nanophotonic devices. In the past, the real part of the refractive index of materials has remained the focus for designing novel devices. The absorption, or imaginary index, was tolerated as an undesirable effect. However, a clever distribution of imaginary index of materials offers an additional degree of freedom for designing nanophotonic devices. Non-Hermitian optics provides a unique opportunity to take advantage of absorption losses in materials to enable unconventional physical effects. Typically occurring near energy degeneracies called exceptional points, these effects include enhanced sensitivity, unidirectional invisibility, and non-trivial topology. In this work, we leverage plasmonic absorption losses (or imaginary index) as a design parameter for non-Hermitian, passive parity-time symmetric metasurfaces. We show that coupled plasmonic-photonic resonator pairs, possessing a large asymmetry in absorptive losses but balanced radiative losses, exhibit an optical phase transition at an exceptional point and directional scattering. These systems enable new pathways for metasurface design using phase, symmetry, and topology as powerful tools.

1. Introduction

Confining light to deep-subwavelength scale comes at the cost of a large radiative or non-radiative loss [1,2]. Plasmonics has enabled light confinement to nanometer, deep-subwavelength scales but is limited by large absorption losses. A search for alternative materials with lower absorption losses is on [3], and yet, losses remain unavoidable. On the other hand, dielectrics circumvent absorption losses at the expense of poor nanoscale light confinement. Combining the positive aspects of plasmonics and dielectrics would enable many nano-optical applications. Such efforts require a design platform where absorption losses in materials can be considered as a design parameter. Non-Hermitian physics offers such a design framework [4–6]. Also, non-Hermitian optics unlocks many unconventional physical effects, including interesting phase transitions [7,8], directionality [9–11], and non-trivial topological properties [12–18]. Using the principles of non-Hermitian optics, we demonstrate a plasmonic-photonic hybrid metasurface that achieves the best of plasmonics and dielectrics, i.e. deep-subwavelength light confinement and low absorption loss.

Non-Hermitian devices have been demonstrated in the super-wavelength scale in the past [4–6]. However, their implementation at deep-subwavelength scales is challenging. Increased radiative losses at the nanoscale limit the achievable quality factors. Despite these challenges, several recent reports have demonstrated non-Hermitian physics in plasmonic systems [19–21]. However, their design principles are yet to be elucidated. Here, we describe a general method to realize non-Hermitian metasurfaces using image resonators in a plasmonic ground plane. This design may be scaled across visible, near-infrared, and mid-infrared spectral ranges. Also, for applications that demand transmission through the metasurface, we show that the image resonator in the ground plane may be replaced by a real resonator to achieve the same passive PT-symmetric behavior.

#428469 https://doi.org/10.1364/OME.428469
Journal © 2021 Received 3 May 2021; revised 17 Jun 2021; accepted 17 Jun 2021; published 24 Jun 2021

Optical Materials EXPRESS

2. Non-Hermitian physics and parity-time symmetry

In quantum mechanics, Hermiticity is usually assumed, implying a closed system. Hermitian systems exhibit energy conservation, real eigenvalues, and physically meaningful observables. If physical systems are allowed to exchange energy with their environments, these properties are no longer guaranteed. Such open or non-Hermitian systems generally have complex eigenvalues and may exhibit exceptional points [4–6]. At exceptional points, eigenvalues become degenerate and eigenmodes skew together severely [22]. Systems tuned to an exceptional point are extremely sensitive to perturbations [7,21,23]. Further, non-Hermitian systems exhibit chiral [24–26] and non-trivial topological properties [12–18].

Systems that respect parity-time (PT) symmetry are one exciting class of non-Hermitian systems [27]. PT-symmetric systems exhibit exceptional points and phase transitions between weakly and strongly coupled regimes. Such true PT-symmetric systems require balanced loss and gain [7]. Since implementing optical gain is hard in nanophotonics, we consider the passive version of a PT-symmetric system [28]. The simplest passive version of a PT-symmetric Hamiltonian is given below (Eq. (1)).

$$\hat{H} = \begin{bmatrix} \omega_0 & \kappa \\ \kappa & \omega_0 + i\gamma \end{bmatrix} \tag{1}$$

This Hamiltonian describes a lossless resonator coupled to a lossy resonator with damping γ, as shown in Fig. 1(A). By tuning the coupling constant κ, the system may be brought through a phase transition. For small κ, in the PT-broken (weakly coupled) regime, the real part of eigenvalues are degenerate and the imaginary parts are split. For large κ, in the PT-symmetric (strongly coupled) regime, the real part of eigenvalues split and the imaginary parts are degenerate. At the phase transition between these two regimes, the eigenvalues become fully degenerate at an exceptional point. The eigenvectors also skew together and become degenerate, and the system becomes defective. This eigenvalue evolution is depicted in Fig. 1(a).

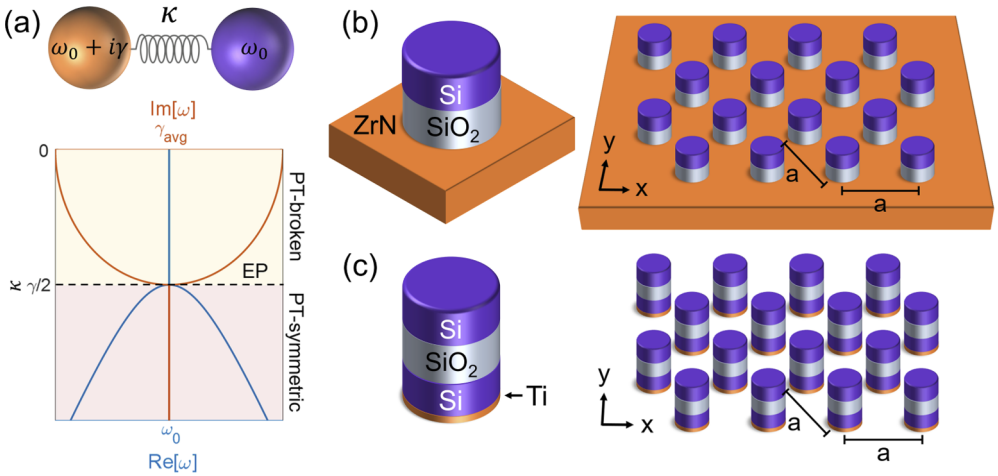

Fig. 1. Overview of passive PT-symmetric metasurfaces. (a) Basic model of coupled resonators and eigenvalue spectrum, showing PT phase transition. Schematic of a passive PT-symmetric metasurface consisting of (b) silicon nanocylinder array coupled to a metal ground plane, (c) an array of silicon nanocylinder dimers. A 1 nm thin layer of titanium is added to the bottom layer to induce loss.

Optical Materials EXPRESS

Recently, several experimental demonstrations of non-Hermitian nanophotonics were reported in the near IR and visible [19–21]. These works induced exceptional points in nanoscale systems by coupling localized dielectric modes to lossy image charges in a metal ground plane [19] or breaking spatial symmetry in periodic plasmonic nanobars [20,21]. Here, we elucidate the design methodology for such parity-time symmetric, non-Hermitian metasurfaces. We design metasurfaces based on (1) engineering localized, quasi-bound states in the continuum and (2) coupling plasmonic and dielectric resonators with very different absorption losses but equal radiative losses.

3. Passive PT-symmetric metasurface design

Nanophotonic devices consist of two kinds of losses, radiative and absorptive. In the simple Hamiltonian of Eq. (1), the effects of radiation are not explicitly considered. A scattering matrix model of the system suggests that the passive version of PT-symmetry requires a large asymmetry in absorption loss [19]. In addition, the radiative losses of the two resonators must be balanced [21]. Balanced radiative losses ensure balanced excitation of the coupled resonators and thereby allow the PT-symmetric phase transition to be observed. These conditions for passive PT-symmetry in nanophotonic devices make their design challenging.

One simple way to meet the requirements of passive PT-symmetry is to use a plasmonic ground plane coupled to low-loss dielectric modes. A plasmonic ground plane produces the image of the near-lossless resonance mode and thus preserves parity symmetry. The losses in the plasmonic ground plane impart the required asymmetry in absorption. The radiation losses balance naturally due to the imaging by the ground plane. Thus, the conditions for passive PT-symmetry are fully satisfied by a ground plane approach.

The ground plane approach results in passive PT-symmetric behavior in reflection. However, in applications that demand transmission, the image in the ground plane could be replaced by a real identical copy of the dielectric resonator. However, to achieve the asymmetry in absorption, one of the resonators needs to be damped. We implement the damping by adding a thin layer of a lossy metal such as titanium. Such coupled resonator pairs or dimers achieve passive PT-symmetry in transmission.

Here, we use finite-difference time-domain (FDTD Lumerical) simulations to outline the two approaches to design passive PT-symmetric metasurfaces: metal ground plane and dimer arrays. We select subwavelength dielectric cylinders for nearly lossless, high Q resonators. In the first case of the metal ground plane, shown in Fig. 1(b), a nearly lossless silicon resonator is coupled to a lossy metal ground plane [19]. Simulated silicon optical constants are obtained from Palik [29]. Here, image charges induced in the lossy ground plane constitute the lossy resonator, resulting in balanced radiative losses and asymmetric absorption losses. Zirconium nitride is selected for the ground plane material, and its optical constants are obtained from a Drude-Lorentz model with parameters extracted from ellipsometric measurements provided in [3].

In the second case of dimer array, shown in Fig. 1(c), we couple two identical, nearly lossless, high Q silicon resonators. To induce loss in the bottom resonator, a thin 1 nm layer of titanium is added below the silicon. In both cases, a silica spacer layer between the lossless and lossy resonators is used to vary the coupling. Silica and titanium optical constants are obtained from Palik [29].

To demonstrate passive PT-symmetry, high Q factor resonators are desirable with the requisite absorption loss asymmetry in the resonators. Subwavelength dielectric resonators circumvent the absorption losses of plasmonics but still suffer from large radiative losses, limiting the highest Q factors possible. This limitation on Q factor can be visualized by Fig. 2(a), which shows scattering and absorption cross sections of the magnetic and electric dipole modes for a single silicon nanocylinder. Field profiles given in Fig. 2(a) confirm the nature of these modes. These

Optical Materials EXPRESS

calculations are performed using FDTD (Lumerical) simulations of a single nanocylinder, with perfectly matched layer (PML) boundary conditions.

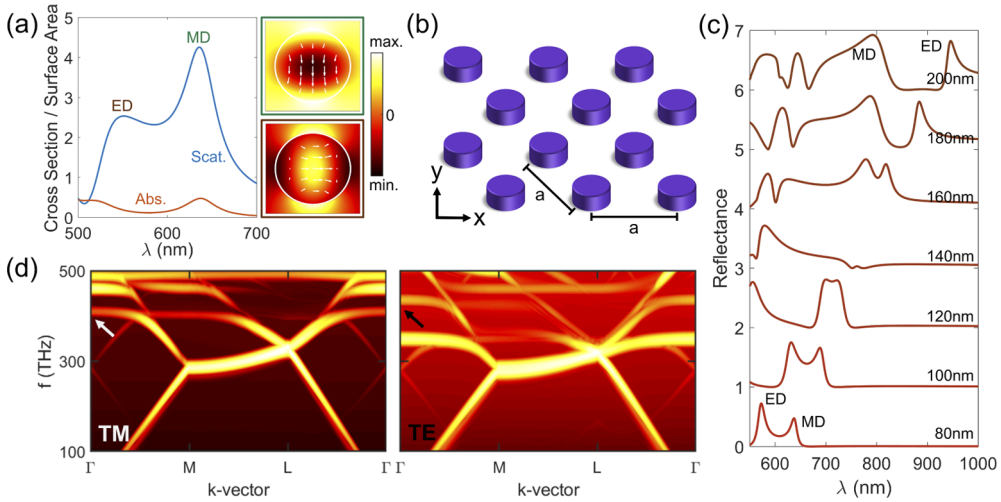

Fig. 2. Localized modes with high quality factor. (a) scattering and absorption cross sections of single silicon cylinder with height = 120 nm and radius = 80 nm, where radiative losses limit achievable Q factors. Right: XY-plane field profiles of magnetic (Re[Hy], green border) and electric (Re[Ex], brown border) dipole modes, (b) schematic of hexagonal array of silicon cylinders with periodicity a = 600 nm, height = 120 nm, and radius = 120 nm, (c) reflectance of array for normally incident, x-polarized input and radius from 80 nm to 200 nm, showing crossing of electric and magnetic dipole modes, (d) TM and TE bandstructure showing flat band near Γ point for silicon resonator array (periodicity a = 600 nm, height = 120 nm, and radius = 120 nm).

One way to overcome the challenge of large radiative losses is by invoking the concept of bound states in the continuum (BIC). BIC modes have theoretically infinite Q factors and do not couple to free-space radiating waves [30]. True BICs are ideal mathematical objects. However, extremely high quality-factor resonances may be induced through the BIC concept of minimizing coupling to free-space radiation via destructive interference. By continuous tuning of parameters, we design such a quasi-BIC, known as a Friedrich-Wintgen quasi-BIC [31]. First, using full-wave simulations, a silicon nanocylinder is placed in a hexagonal array to reduce in-plane radiative losses, as shown in Fig. 2(b). Then, by tuning the nanocylinder radius, magnetic and electric dipoles are spectrally overlapped, resulting in destructive interference outside of the nanocylinders and a highly localized mode (Fig. 2(c)). The localized nature of these modes is confirmed through calculations of the TE and TM bandstructure of the hexagonal array, which exhibits flat bands near the Γ point (marked by arrows in Fig. 2(d)). Flat bands in reciprocal space correspond to localization in real space. Photonic bandstructure was calculated using FDTD (Lumerical) simulation.

These highly localized, lossless, dielectric resonators may now be coupled to lossy resonators in the configurations proposed in Fig. 3(a, d). In the first case, silicon nanocylinders are coupled to a lossy zirconium nitride ground plane using a silica spacer layer. As the silica spacer layer thickness is tuned from 0-100 nm, the system undergoes a PT-phase transition from the strongly-coupled to weakly-coupled regimes, as shown in Fig. 3(b). For low spacer thicknesses below 60 nm, two absorption peaks are visible. These peaks merge at the exceptional point at 60 nm and remain degenerate in the weakly-coupled regime (spacer thickness above 60 nm). The real part of the eigenvalues remain the same in the weakly-coupled (PT-broken) regime, but

Optical Materials EXPRESS

the imaginary part of eigenvalues splits, resulting in increased Q factor. In the ground plane system, Q factor increases to 40. The same PT-symmetric behavior is observed in the second configuration of two coupled silicon resonators (Fig. 3(e)). In this case, spacer thickness is tuned from 0-200 nm, and Q factor increases to 48 in the weakly-coupled regime.

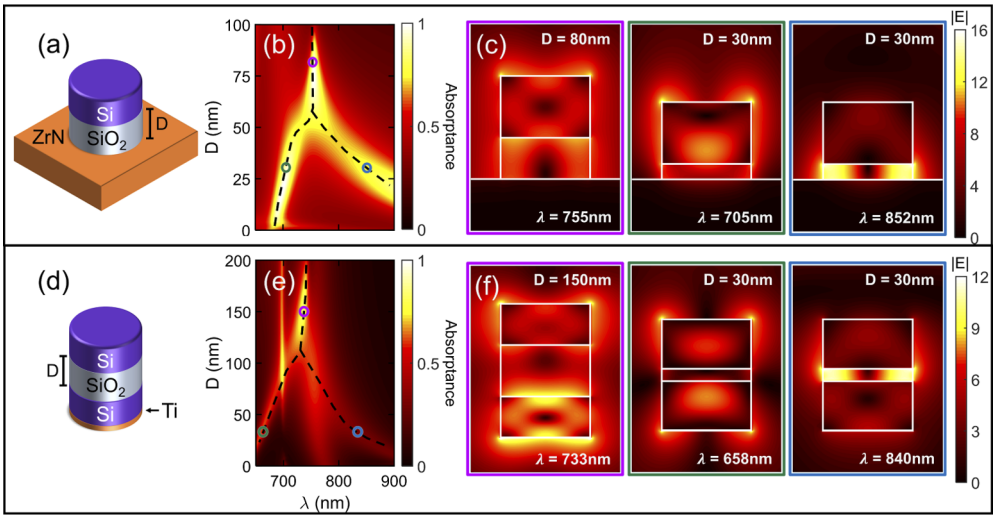

Fig. 3. Plane-wave excitation of different PT-symmetric metasurfaces (a) ground plane system and (d) coupled resonator system schematics, (b, e) absorption spectra showing passive PT-symmetry as spacer thickness D is decreased, (c, f) XZ-plane electric field profiles in PT-symmetric and PT-broken regimes.

The two phases of the PT-symmetric metasurface exhibit qualitatively different energy storage behavior, as shown in the field profiles of Fig. 3(c, f). In the PT-symmetric phase, the modes at the two resonance frequencies are, through mode hybridization, either symmetric or anti-symmetric. The quasi-BIC mode hybridizes with its image in the ground plane case and a second quasi-BIC in the coupled dimer case. This results in an anti-symmetric mode at higher energy and symmetric mode at lower energy. In the symmetric mode, fields in the two resonators are in phase, resulting in large field in the spacer. In the anti-symmetric mode, fields in the individual resonators are out of phase, resulting in low fields in the spacer. Energy oscillates between the strongly coupled resonators in the PT-symmetric phase [19]. In the PT-broken phase, energy storage is largely confined to one resonator in both configurations.

Further, the optical phase transition in the passive PT-symmetric system exhibits an interesting scattering property. In the strongly coupled or PT-symmetric phase, the energy is nearly equally distributed between the resonators, making them scatter equally. However, the asymmetric modes in the weakly coupled or broken-symmetry phase make the scattering directional [9,11,25,32,33].

To explore the directional scattering phenomenon of non-Hermitian metasurfaces, we study the behavior of quantum emitters placed in the near field of the system of coupled dielectric slabs (given in Fig. 1(c)). Coherent, x-polarized dipoles are placed 5 nm above or below the lossless or lossy resonators. Forward and back-scattered powers are measured using power monitors.

As shown in Fig. 4(a, b), we find that the radiative Purcell enhancement of emitters above and below the metasurface is symmetric for low spacer thickness in the PT-symmetric regime. As spacer thickness is increased (and coupling decreases), the device approaches the exceptional point, and radiative Purcell enhancement increases for the dipole on the lossless side as compared to the lossy side. In the PT-broken regime, this asymmetric behavior is very pronounced. Radiative Purcell enhancement is calculated by integrating power radiated above and below the

Optical Materials EXPRESS

coupled silicon arrays for a single unit cell and normalizing against the power radiated above and below an equivalent infinite array of coherent dipole emitters in vacuum.

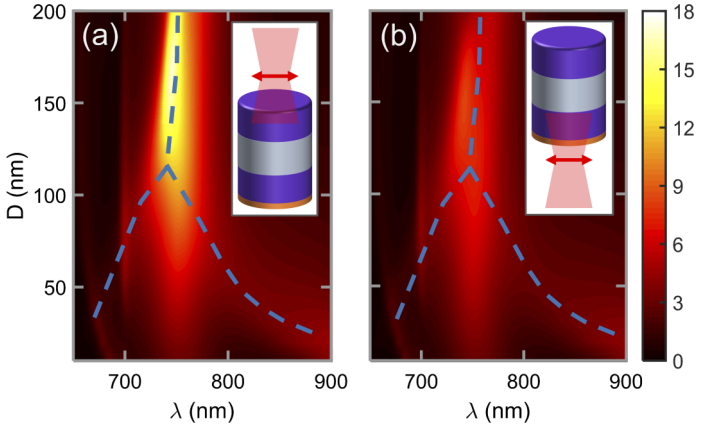

Fig. 4. Coupled resonator system: asymmetric scattering of quantum emitters Radiative Purcell enhancement for x-polarized dipoles (a) on the lossless or (b) on the lossy sides of the metasurface.

The interesting phenomena associated with non-Hermitian systems are not limited to the optical phase transition and directional scattering. In coupled systems more complicated than a dimer, such as a four-resonator system, more interesting phenomena arise. Such higher-order systems could exhibit interesting topological properties [34,35]. Our ground-plane design serves as an easy platform to study such higher-order passive PT-symmetric nanophotonic devices.

The ground-plane design shown in Fig. 1(b), supports vertical dipole modes at the same frequency. For normally incident plane-wave excitation, only horizontal modes are excited in the resonator. At oblique incidences, vertical modes are also excited. Vertical modes not only couple to their corresponding image mode in the metal ground plane but also to the horizontal dipole mode. Thus, a coupled four-resonator passive PT-symmetry is possible in our design. While the coupling between the modes and their images is controlled by the dielectric spacer thickness, the incident angle controls the vertical-horizontal mode coupling.

This new system is depicted in Fig. 5(a). We may model its behavior by a 4x4 Hamiltonian, given in Eq. (2). The Hamiltonian contains coupling terms between the vertical and horizontal modes (κ_θ) and each dielectric mode with its lossy image (κ_1, κ_2). Coupling between dielectric modes and their corresponding image charges is, again, tuned using spacer thickness.

$$\hat{H} = \begin{bmatrix} \omega_0 & \kappa_1 & \kappa_\theta & 0 \\ \kappa_1 & \omega_0 + i\gamma & 0 & \kappa_\theta \\ \kappa_\theta & 0 & \omega_0 & \kappa_2 \\ 0 & \kappa_\theta & \kappa_2 & \omega_0 + i\gamma \end{bmatrix} \tag{2}$$

The eigenvalues of the 4x4 Hamiltonian are plotted in Fig. 5(b) and exhibit phenomena such as exceptional lines. Figure 5(c) shows the real part of eigenvalues of the Hamiltonian for a constant vertical-horizontal coupling (κ_θ). This corresponds to varying spacer thickness between the two resonators with a fixed incident angle excitation. Here, the eigenvalues exhibit PT-symmetric behavior and PT-phase transition at two branch points. Figure 5(d) shows the real part of eigenvalues for constant plasmonic-photonic coupling (κ_1, κ_2). This corresponds to fixing the spacer thickness and varying incident angle of light. In this case, two exceptional points may

Optical Materials EXPRESS

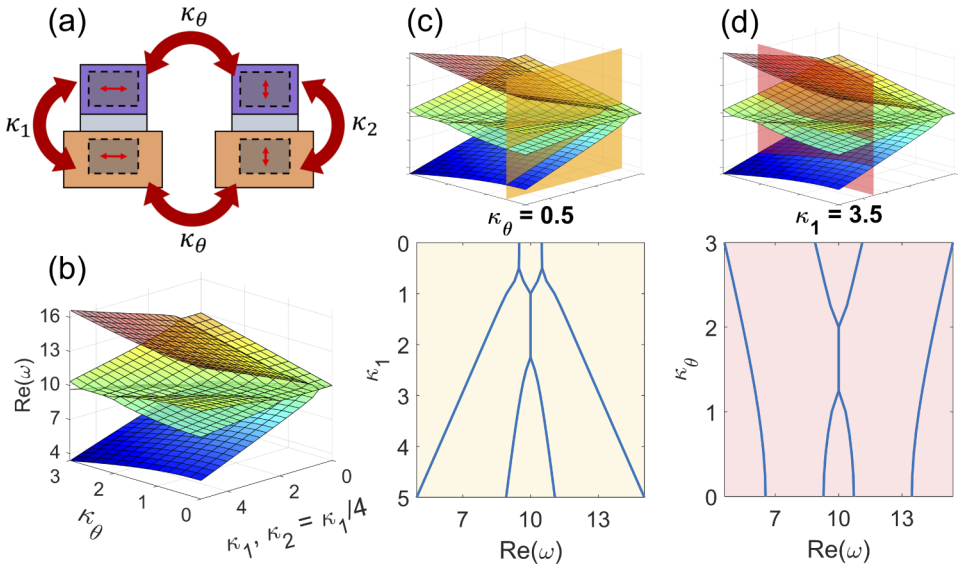

Fig. 5. Ground plane system: coupling between horizontal and vertical modes unlocks topological effects (a) schematic showing coupling between vertical and horizontal modes and their image charges, (b) eigenvalue surface for 4x4 Hamiltonian given in Eqn. 2, with $\omega_0 = 10$, $\kappa_2 = \kappa_1/4$, $\gamma = 1$, (c) Real part of eigenvalues for constant vertical-horizontal coupling ($\kappa_\theta = 0.5$), (d) Real part of eigenvalues for constant plasmonic-photonic coupling ($\kappa_1 = 3.5$).

be observed as vertical-horizontal coupling increases. A full k-space plot of the modes in the system leads to topological features such as exceptional concentric rings [36].

4. Summary and conclusion

In summary, we demonstrated the design principles of non-Hermitian, plasmonic-dielectric metasurfaces. In particular, we showed two approaches to realize passive PT-symmetry: using a ground plane and a dimer array. We leveraged absorption losses in plasmonics as a design parameter for non-Hermitian metasurfaces based on nearly lossless, localized, dielectric modes. Our results highlighted the optical phase transition, directional scattering, and topological features in passive PT-symmetric metasurfaces. Non-Hermitian nanophotonics provides a framework to engineer optical losses in deep-subwavelength systems, and many more phenomena remain to be explored in such systems. These include many-body effects in nanophotonic devices, including superradiance [37] and non-trivial topology [12–18]. The design principles discussed here for plasmonic-dielectric metasurfaces could enable devices with unprecedented functionalities for emerging applications in sensing, nanoscale light sources, and switches.

Funding. National Science Foundation (ECCS 1935446); Army Research Office (W911NF2120031).

Disclosures. The authors declare no conflicts of interest.

Data availability. Data underlying the results presented in this paper are not publicly available at this time but may be obtained from the authors upon reasonable request.

References

1. A. Boltasseva and H. A. Atwater, "Low-loss plasmonic metamaterials," Science **331**(6015), 290–291 (2011).
2. D. G. Baranov, D. A. Zuev, S. I. Lepeshov, O. V. Kotov, A. E. Krasnok, A. B. Evlyukhin, and B. N. Chichkov, "All-dielectric nanophotonics: the quest for better materials and fabrication techniques," Optica **4**(7), 814–825 (2017).

Optical Materials EXPRESS

3. G. V. Naik, V. M. Shalaev, and A. Boltasseva, "Alternative plasmonic materials: beyond gold and silver," Adv. Mater. **25**(24), 3264–3294 (2013).
4. L. Feng, R. El-Ganainy, and L. Ge, "Non-Hermitian photonics based on parity–time symmetry," Nat. Photonics **11**(12), 752–762 (2017).
5. R. El-Ganainy, K. G. Makris, M. Khajavikhan, Z. H. Musslimani, S. Rotter, and D. N. Christodoulides, "Non-Hermitian physics and PT symmetry," Nat. Phys. **14**(1), 11–19 (2018).
6. Ş. K. Özdemir, S. Rotter, F. Nori, and L. Yang, "Parity–time symmetry and exceptional points in photonics," Nat. Mater. **18**(8), 783–798 (2019).
7. B. Peng, Ş. K. Özdemir, F. Lei, F. Monifi, M. Gianfreda, G. L. Long, S. Fan, F. Nori, C. M. Bender, and L. Yang, "Parity–time-symmetric whispering-gallery microcavities," Nat. Phys. **10**(5), 394–398 (2014).
8. H. Alaeian and J. A. Dionne, "Parity-time-symmetric plasmonic metamaterials," Phys. Rev. A **89**(3), 033829 (2014).
9. Z. Lin, H. Ramezani, T. Eichelkraut, T. Kottos, H. Cao, and D. N. Christodoulides, "Unidirectional invisibility induced by $\mathcal{PT}$-symmetric periodic structures," Phys. Rev. Lett. **106**(21), 213901 (2011).
10. L. Feng, Z. J. Wong, R.-M. Ma, Y. Wang, and X. Zhang, "Single-mode laser by parity-time symmetry breaking," Science **346**(6212), 972–975 (2014).
11. H. Alaeian and J. A. Dionne, "Non-Hermitian nanophotonic and plasmonic waveguides," Phys. Rev. B **89**(7), 075136 (2014).
12. B. Midya, H. Zhao, and L. Feng, "Non-Hermitian photonics promises exceptional topology of light," Nat. Commun. **9**(1), 2674 (2018).
13. B. Zhen, C. W. Hsu, Y. Igarashi, L. Lu, I. Kaminer, A. Pick, S.-L. Chua, J. D. Joannopoulos, and M. Soljačić, "Spawning rings of exceptional points out of Dirac cones," Nature **525**(7569), 354–358 (2015).
14. C. Poli, M. Bellec, U. Kuhl, F. Mortessagne, and H. Schomerus, "Selective enhancement of topologically induced interface states in a dielectric resonator chain," Nat. Commun. **6**(1), 6710 (2015).
15. S. Weimann, M. Kremer, Y. Plotnik, Y. Lumer, S. Nolte, K. G. Makris, M. Segev, M. C. Rechtsman, and A. Szameit, "Topologically protected bound states in photonic parity–time-symmetric crystals," Nat. Mater. **16**(4), 433–438 (2017).
16. H. Zhao, X. Qiao, T. Wu, B. Midya, S. Longhi, and L. Feng, "Non-Hermitian topological light steering," Science **365**(6458), 1163–1166 (2019).
17. S. Weidemann, M. Kremer, T. Helbig, T. Hofmann, A. Stegmaier, M. Greiter, R. Thomale, and A. Szameit, "Topological funneling of light," Science **368**(6488), 311–314 (2020).
18. K. Wang, A. Dutt, K. Y. Yang, C. C. Wojcik, J. Vučković, and S. Fan, "Generating arbitrary topological windings of a non-Hermitian band," Science **371**(6535), 1240–1245 (2021).
19. C. F. Doiron and G. V. Naik, "Non-Hermitian selective thermal emitters using metal–semiconductor hybrid resonators," Adv. Mater. **31**(44), 1904154 (2019).
20. H. M. Leung, W. Gao, R. Zhang, R. Zhang, Q. Zhao, X. Wang, C. T. Chan, J. Li, J. Li, W. Y. Tam, and W. Y. Tam, "Exceptional point-based plasmonic metasurfaces for vortex beam generation," Opt. Express **28**(1), 503–510 (2020).
21. J.-H. Park, A. Ndao, W. Cai, L. Hsu, A. Kodigala, T. Lepetit, Y.-H. Lo, and B. Kanté, "Symmetry-breaking-induced plasmonic exceptional points and nanoscale sensing," Nat. Phys. **16**(4), 462–468 (2020).
22. C. M. Bender, M. V. Berry, and A. Mandilara, "Generalized PT symmetry and real spectra," J. Phys. A: Math. Gen. **35**(31), L467–L471 (2002).
23. J. Wiersig, "Sensors operating at exceptional points: General theory," Phys. Rev. A **93**(3), 033809 (2016).
24. B. Peng, Ş. K. Özdemir, M. Liertzer, W. Chen, J. Kramer, H. Yılmaz, J. Wiersig, S. Rotter, and L. Yang, "Chiral modes and directional lasing at exceptional points," Proc. Natl. Acad. Sci. U. S. A. **113**(25), 6845–6850 (2016).
25. H. Alaeian and J. A. Dionne, "Controlling electric, magnetic, and chiral dipolar emission with PT-symmetric potentials," Phys. Rev. B **91**(24), 245108 (2015).
26. P. Miao, Z. Zhang, J. Sun, W. Walasik, S. Longhi, N. M. Litchinitser, and L. Feng, "Orbital angular momentum microlaser," Science **353**(6298), 464–467 (2016).
27. C. M. Bender and S. Boettcher, "Real spectra in non-hermitian hamiltonians having PT symmetry," Phys. Rev. Lett. **80**(24), 5243–5246 (1998).
28. A. Guo, G. J. Salamo, D. Duchesne, R. Morandotti, M. Volatier-Ravat, V. Aimez, G. A. Siviloglou, and D. N. Christodoulides, "Observation of $\mathcal{PT}$-symmetry breaking in complex optical potentials," Phys. Rev. Lett. **103**(9), 093902 (2009).
29. E. D. Palik, *Handbook of Optical Constants of Solids*, vol. 3 (Academic Press, 1998), Doi: 10.1016/C2009-0-20920-2.
30. C. W. Hsu, B. Zhen, A. D. Stone, J. D. Joannopoulos, and M. Soljačić, "Bound states in the continuum," Nat. Rev. Mater. **1**(9), 16048 (2016).
31. T. Lepetit, E. Akmansoy, J.-P. Ganne, and J.-M. Lourtioz, "Resonance continuum coupling in high-permittivity dielectric metamaterials," Phys. Rev. B **82**(19), 195307 (2010).
32. N. S. Nye, A. E. Halawany, C. Markos, M. Khajavikhan, and D. N. Christodoulides, "Flexible $\mathcal{PT}$-symmetric optical metasurfaces," Phys. Rev. Appl. **13**(6), 064005 (2020).
33. A. Manjavacas, "Anisotropic optical response of nanostructures with balanced gain and loss," ACS Photonics **3**(7), 1301–1307 (2016).
34. H. Hodaei, A. U. Hassan, S. Wittek, H. Garcia-Gracia, R. El-Ganainy, D. N. Christodoulides, and M. Khajavikhan, "Enhanced sensitivity at higher-order exceptional points," Nature **548**(7666), 187–191 (2017).

Optical Materials EXPRESS

35. A. Kodigala, T. Lepetit, and B. Kanté, "Exceptional points in three-dimensional plasmonic nanostructures," Phys. Rev. B **94**(20), 201103 (2016).
36. H. Wang, B. Xie, S. K. Gupta, X. Zhu, L. Liu, X. Liu, M. Lu, and Y. Chen, "Exceptional concentric rings in a non-Hermitian bilayer photonic system," Phys. Rev. B **100**(16), 165134 (2019).
37. L. Zhang, G. S. Agarwal, W. P. Schleich, and M. O. Scully, "Hidden $\mathcal{PT}$ symmetry and quantization of a coupled-oscillator model of quantum amplification by superradiant emission of radiation," Phys. Rev. A **96**(1), 013827 (2017).